International Forum on Aeroelasticity and Structural Dynamics
IFASD 2017
25-28 June 2017, Como, Italy

COMPUTING DERIVATIVES IN NONLINEAR AEROELASTICITY USING ALGORITHM DIFFERENTIATION

Ruben Sanchez[1] **and Rafael Palacios**[1]

[1]Department of Aeronautics, Imperial College London
South Kensington Campus, London SW7 2AZ, United Kingdom
r.palacios@imperial.ac.uk

Keywords: fluid-structure interaction, multidisciplinary optimization, algorithmic differentiation, adjoint sensititivities, geometrically-nonlinear structures, viscous flows

Abstract: This paper introduces a new method to calculate design sensitivities in high-fidelity fluid-structural interactions problems. As the intended application is on aeroelastic systems, characterized by many design variables and a small number of objective functions, gradients are computed from the fully-coupled adjoint equation. This is cast here as an iterated sequence for which convergence is guaranteed. The system is finally obtained using algorithm differentiation on the fully-coupled primal problem and its solution is then sought using a block Gauss-Seidel method, which preserves the partitioned structure of the primal coupled solver. This solution architecture has been implemented in the open-source SU2 software suite for the solution of industrial-scale aeroelastic optimization problems with viscous fluids and structures with nonlinear geometric and material response.

1 INTRODUCTION

Our interest here is in high-fidelity computational solutions for nonlinear aeroelastic design. Computational methods in fluid-structure-interaction (FSI) are by now mature enough to predict coupled responses involving complex physics and, in particular, nonlinear response in the structure (albeit still with a relatively large computational overhead). High-fidelity optimization, however, is mostly done at the discipline level [1,2], and, for coupled problems the vast majority of the published research is restricted to either linear structural behaviour [3] or potential-flow aerodynamics [4]. For fully nonlinear aeroelastic systems (that is, nonlinear structure and viscous flow), optimization strategies have typically been based on either monolithic simulation environments [5], which bring restrictions in geometrical complexity, or on the differentiation of the direct equations [6], which puts a limit to the number of design parameters in the problem.

Adjoint methods are shown to be an efficient approach for problems with a large number of design variables, and they are nowadays the basis for most large-scale wing aerodynamic and aeroelastic optimization solutions. The main challenge is that the adjoint equations are built on an exact linearization of the primal problem, which can be difficult to obtain analytically for problems with complex physics. To overcome this, algorithmic differentiation (AD) strategies [7] have been developed, in which the derivatives are obtained automatically by manipulation of the computer code that solves the primal problem. AD is normally used to compute a subset of the derivatives for discrete adjoints in FSI applications [3]. Instead, we propose a general approach that consistently applies AD to a full partitioned FSI solver, using the framework

defined by Albring [8] for aerodynamic and aeroacoustic optimization. We will show in this work that this approach is suitable to compute accurate gradients for FSI problems involving viscous flows and non-linear solid mechanics with a moderate computational cost and memory requirements.

2 METHODOLOGY

2.1 FSI formulation

We have implemented a partitioned, strongly-coupled FSI solver in the open-source SU2 software suite [1,9]. The general solution is based on a time-marching algorithm, although here we will restrict ourselves to steady-state problem for the applications in design optimization. The solution of the primal (or direct) problem is based on a three-field formulation [10], as shown in Fig. 1. The fluid domain is solved using a finite-volume discretization of the compressible Navier-Stokes equations, which will be symbolically represented as $\mathscr{F}(\mathbf{w}, \mathbf{z}) = \mathbf{0}$. Here, $\mathbf{w} = (\rho_f, \rho_f \mathbf{v}, \rho_f e)$ is the flow conservative variable vector, where ρ_f is the fluid density, $\mathbf{v}$ is the vector of flow velocities in a three-dimensional Cartesian coordinate system, and e is the total energy of the flow per unit mass. Finally, $\mathbf{z}$ is the position of the fluid mesh nodes of the finite-volume discretization.

The structural domain is solved through a finite-element equations of the finite-strain formulation of nonlinear solid mechanics, which will be analogously written as $\mathscr{S}(\mathbf{u}, \mathbf{z}, \mathbf{w}) = \mathbf{0}$, where $\mathbf{u}$ be the vector of displacements of the structural nodes. The third field is the mesh, for which large deformations are allowed by means of a pseudo-elastic linear problem [11]. The coupling is defined at the interface through a consistent transfer of tractions λ_T from fluid to structure, and of the displacements, u_Γ from structure to fluid. The direct problem is solved iteratively using a Block-Gauss-Seidel method with approximated Jacobians.

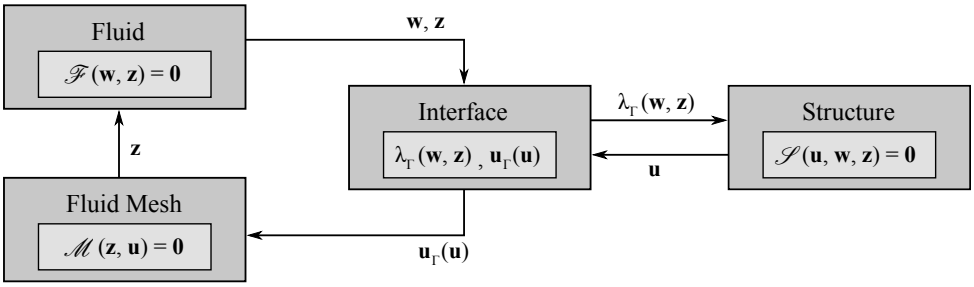

Figure 1: Three-field formulation for Fluid-Structure Interaction problems

To obtain the coupled sensitivities, the three sub-problems are first rewritten in the form of fixed-point iterations. This is easily obtained by defining the iteration sequence as the solution of the Newton method on the original equations, noting that only an approximated Jacobian is required for convergence. If $(\mathbf{u}^*, \mathbf{w}^*, \mathbf{z}^*)$ denote the (converged) equilibrium solution of the primal problem, the three subproblems defined above are rewritten as

$$\begin{aligned} \mathscr{S}(\mathbf{u}^*, \mathbf{z}^*, \mathbf{w}^*, \boldsymbol{\alpha}) = \mathbf{0} \Leftrightarrow \mathbf{u}^* = \mathbf{S}(\mathbf{u}^*, \mathbf{z}^*, \mathbf{w}^*, \boldsymbol{\alpha}), \\ \mathscr{F}(\mathbf{w}^*, \mathbf{z}^*, \boldsymbol{\alpha}) = \mathbf{0} \Leftrightarrow \mathbf{w}^* = \mathbf{G}(\mathbf{w}^*, \mathbf{z}^*, \boldsymbol{\alpha}), \\ \mathscr{M}(\mathbf{u}^*, \mathbf{z}^*) = \mathbf{0} \Leftrightarrow \mathbf{z}^* = \mathbf{M}(\mathbf{u}^*, \boldsymbol{\alpha}) \end{aligned} \tag{1}$$

where we have explicitly identified the design variables $\boldsymbol{\alpha}$, which, in general, may be parameters acting on any of the three fields in the problem. We can now define the following optimization

problem results in a suitable range of the design and state parameters,

$$\begin{aligned} \min \quad & J\left(\mathbf{w}(\boldsymbol{\alpha}), \mathbf{z}(\boldsymbol{\alpha}), \mathbf{u}(\boldsymbol{\alpha}), \boldsymbol{\alpha}\right) \\ \text{subject to} \quad & \mathbf{u}(\boldsymbol{\alpha}) = \mathbf{S}\left(\mathbf{u}(\boldsymbol{\alpha}), \mathbf{w}(\boldsymbol{\alpha}), \mathbf{z}(\boldsymbol{\alpha}), \boldsymbol{\alpha}\right) \\ & \mathbf{w}(\boldsymbol{\alpha}) = \mathbf{G}\left(\mathbf{w}(\boldsymbol{\alpha}), \mathbf{z}(\boldsymbol{\alpha}), \boldsymbol{\alpha}\right) \\ & \mathbf{z}(\boldsymbol{\alpha}) = \mathbf{M}\left(\mathbf{u}(\boldsymbol{\alpha}), \boldsymbol{\alpha}\right) \end{aligned} \tag{2}$$

To seek numerical solutions of this problem, we will first define the Lagrangian of the coupled problem, which can be written as

$$\begin{aligned} L(\boldsymbol{\alpha}, \mathbf{u}, \bar{\mathbf{u}}, \mathbf{w}, \bar{\mathbf{w}}, \mathbf{z}, \bar{\mathbf{z}}) = & J(\mathbf{u}, \mathbf{w}, \mathbf{z}, \boldsymbol{\alpha}) \\ & + \bar{\mathbf{w}}^T[\mathbf{G}(\mathbf{w}, \mathbf{z}, \boldsymbol{\alpha}) - \mathbf{w}] \\ & + \bar{\mathbf{u}}^T[\mathbf{S}(\mathbf{u}, \mathbf{w}, \mathbf{z}, \boldsymbol{\alpha}) - \mathbf{u}] \\ & + \bar{\mathbf{z}}^T[\mathbf{M}(\mathbf{u}, \boldsymbol{\alpha}) - \mathbf{z}] \end{aligned} \tag{3}$$

where the Lagrange multipliers $(\bar{\mathbf{u}}, \bar{\mathbf{w}}, \bar{\mathbf{z}})$ are the adjoint variables associated to the primal variables in the problem. Note first that the governing equations in the right-hand side of the equations are identically satisfied for each evaluation of the design variable, $\boldsymbol{\alpha}$. Consequently, the total derivative of the Lagrangian corresponds to $\frac{dL}{d\boldsymbol{\alpha}} = \frac{dJ}{d\boldsymbol{\alpha}}$, which allows to write the gradient of the objective function in terms of the adjoint variables, as

$$\frac{\mathrm{d}J}{\mathrm{d}\boldsymbol{\alpha}} = \frac{\partial J}{\partial \boldsymbol{\alpha}} + \bar{\mathbf{u}}^T \frac{\partial \mathbf{S}}{\partial \boldsymbol{\alpha}} + \bar{\mathbf{w}}^T \frac{\partial \mathbf{G}}{\partial \boldsymbol{\alpha}} + \bar{\mathbf{z}}^T \frac{\partial \mathbf{M}}{\partial \boldsymbol{\alpha}} \tag{4}$$

The solution to the optimization problem is obtained by differentiating (3) with respect to states, adjoints and design variables, which yields the well-known Karush-Kuhn-Tucker (KKT) conditions [12]. In particular, differentiating with respect to the structural variables, $\mathbf{u}$, the flow conservative variables, $\mathbf{w}$, and the mesh variables $\mathbf{z}$, we obtain the fixed-point equations for their corresponding adjoints, as

$$\begin{aligned} \bar{\mathbf{u}}^T &= \frac{\partial J}{\partial \mathbf{u}} + \bar{\mathbf{u}}^T \frac{\partial \mathbf{S}}{\partial \mathbf{u}} + \bar{\mathbf{z}}^T \frac{\partial \mathbf{M}}{\partial \mathbf{u}} \\ \bar{\mathbf{w}}^T &= \frac{\partial J}{\partial \mathbf{w}} + \bar{\mathbf{w}}^T \frac{\partial \mathbf{G}}{\partial \mathbf{w}} + \bar{\mathbf{u}}^T \frac{\partial \mathbf{S}}{\partial \mathbf{w}} \\ \bar{\mathbf{z}}^T &= \frac{\partial J}{\partial \mathbf{z}} + \bar{\mathbf{w}}^T \frac{\partial \mathbf{G}}{\partial \mathbf{z}} + \bar{\mathbf{u}}^T \frac{\partial \mathbf{S}}{\partial \mathbf{z}} \end{aligned} \tag{5}$$

Combining (4) and (5) we can now evaluate the sensitivity of the objective function with respect to the design parameters, around feasible solutions of the FSI problem. The challenge is to obtain the partial derivatives of the fixed-point operators, which were defined in (1), with respect to the problem variables. This is normally quite challeging challenging for the cross-terms (e.g. the derivative of the structure operator with respect to the fluid variables, $\frac{\partial \mathbf{S}}{\partial \mathbf{w}}$), but also for the block diagonal terms (e.g. $\frac{\partial \mathbf{S}}{\partial \mathbf{u}}$) when also with complex governing equations in either the solid or the fluid subdomains. To overcome this, solution of (1) will be sought here through algorithmic differentiation, as discussed in the following section.

2.2 Solution of the adjoint equations using algorithmic differentiation

The solution process is based on the strategy developed by Albring *et al.* [8] for the solution of the adjoint equations in aerodynamic and aeroacoustics problems, and that is already implemented in SU2. To facilitate the discussion, consider only the structural adjoint problem, for which the solution process is shown in Fig. 2.

1. The starting point is the solution of the direct problem, $\mathbf{u}^*$, which can be obtained using standard process of minimisation of the residual equations (not necessarily via a fixed-point iteration).
2. Then a single iteration on the fixed-point equation is carried out, that is, $\mathbf{u}^* + \Delta\mathbf{u}^* = \mathbf{S}\left(\mathbf{u}^*, \boldsymbol{\alpha}\right) \approx \mathbf{u}^*$.
3. The jacobian of the function, $\frac{\partial \mathbf{S}}{\partial \mathbf{u}}$ can be now directly obtained usign the direct mode of AD. However, as the objective is to compute the adjoint, the reverse mode will be used instead. In that case, all the operations are recorded instead and the displacement field is registered as the input variables to the AD. The recording step is done using expression templates [13], which is a highly efficient strategy with minimum computational and memory overheads.
4. Before stopping the recording, one evaluation of the cost function $J(\mathbf{u}^*, \boldsymbol{\alpha})$ is also recorded, and the structural displacements are also registered as outputs, as the objective is to compute their adjoints $\bar{\mathbf{u}}$.
5. The adjoint variables are now initialized to zero, $\bar{\mathbf{u}}^0$, and fixed-point iterations of the form $\bar{\mathbf{u}}^{n+1} = \frac{\partial J}{\partial \mathbf{u}}^\top + \frac{\partial \mathbf{S}}{\partial \mathbf{u}}^\top \bar{\mathbf{u}}^n = \bar{\mathbf{S}}(\bar{\mathbf{u}}^n)$ are carried using the recorded computational graph until convergence.
6. The resulting adjoint $\bar{\mathbf{u}}$ is then used in (4) (retaining only structural terms) to obtain the sensitivities with respect to the design variables.

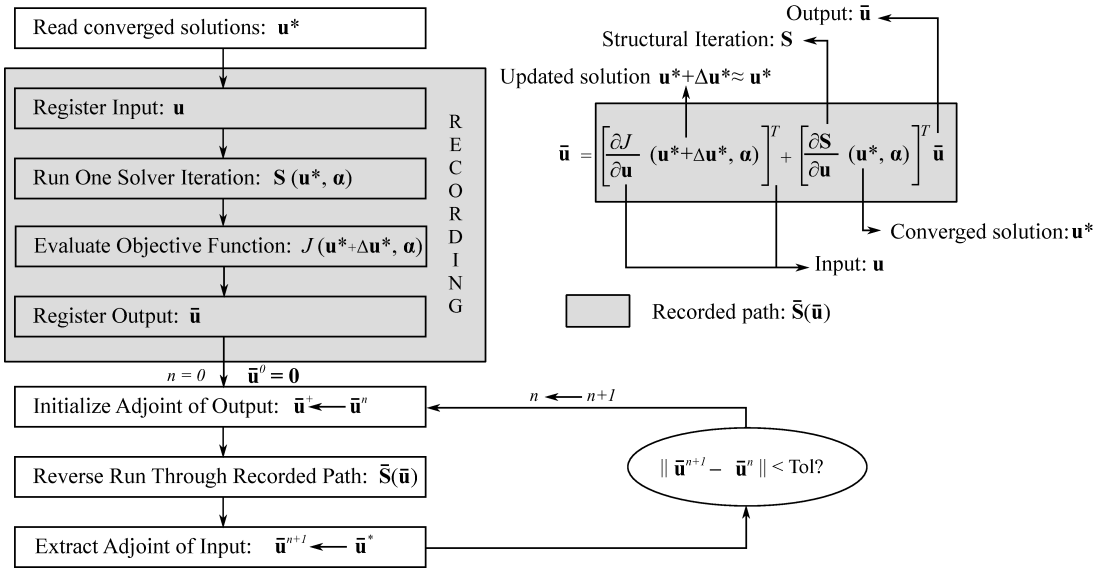

Figure 2: Top-level approach to the structural adjoint calculation using AD

For the coupled problem (5), the solution is sought using an iterative Block-Gauss-Seidel (BGS) procedure, as it was done with the primal solver. The algorithm above then is now repeated for each of the three fixed-point operators **S**, **G**, and **M** and with respect to all its input variables – assuming in each BGS iteration that two out of the three sets of variables $(\mathbf{u}, \mathbf{w}, \mathbf{z})$ are fixed. It can be shown [8] that if the primal equations converge, the adjoint equations will also converge.

Finally, ofnce the adjoint variables $(\bar{\mathbf{u}}, \bar{\mathbf{w}}\bar{\mathbf{z}})$ are obtained, then (4) gives the sensitivities of the objective function with respect to the design variables.

3 NUMERICAL EXAMPLE

We will examplify the methodology introduced above with a flexible cantilever in a low-Reynolds channel flow, as shown in Fig. 3. The design variable is the Young's modulus, $E \in [13 - 28]$ kPa, of the structure, which is modelled using solid elements. The objective will be to achieve a desired shape in the equilibrium condition, which will be obtained with the cost function

$$J(\mathbf{u}) = (\mathbf{u} - \mathbf{u}_{ref})^T \mathbf{C} (\mathbf{u} - \mathbf{u}_{ref}), \tag{6}$$

which will be chosen as $\mathbf{C} = k\mathbf{I}$, $k = 10^6$ and $\mathbf{u}_{ref} = 0$, where k is a penalty factor to avoid scaling effects in the structural domain.

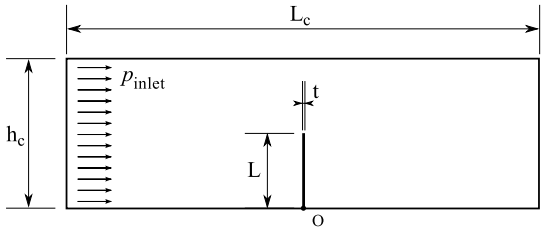

L_c = 20 cm
h_c = 3.2 cm
Re = 10
Ma = 0.2
p_{inlet} = 20.1347 Pa
p_{fs} = 19.5809 Pa
T = 0.0578 K
ρ_f = 1.18 kg/m^3
μ_f = 1.82·10^{-3} kg/m·s

Figure 3: Test case: A very flexible cantilever in a channel flow (L=1.6 cm, t=0.1 cm).

This is a relatively inexpensive computational problem, but that shows the physics of interest. The flow needs to be fully-resolved using the Navier-Stokes equations, while the structure follows a Neo-Hookean material model and displays geometrically-nonlinear effects. As an example of this, the equilibrium conditions for the limit cases, in the range of Young's modulus considered, are shown in Fig. 4. Note that with E = 13 kPa, the amplitude of the tip displacement at the tip is nearly $0.4L$.

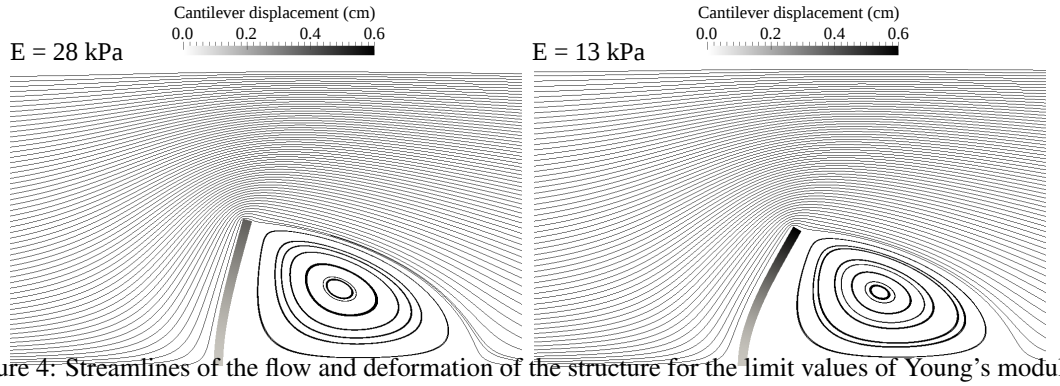

Figure 4: Streamlines of the flow and deformation of the structure for the limit values of Young's modulus.

Finally, in Fig. 5, the objective function, the sensitivity $\mathrm{d}J/\mathrm{d}E$, and the relative error with respect to the *Forward Mode* of AD, which has also been implemented, are shown. The solution with the *Central Differences* scheme is obtained with $h = 0.5$ kPa. As it can be seen, there are minimum differences between all three methods. However, the reverse AD is based on a single simulation and indeed this is the case regardless of the number of design variables. To exemplify this, Fig. 6 shows the sensitivities to Young's modulus on 10 different regions of a cantilever of E=21 kPa. Solutions are obtained again using the reverse mode of AD and central differences, and they agree very well with the forward mode of AD. Note the the central differences requires

21 simulations, the forward-mode 10 simulations, and the reverse mode, only 2 simulations (the iteration to convergence of the primal solver, and the subsequent recording and iterations of the adjoint solver).

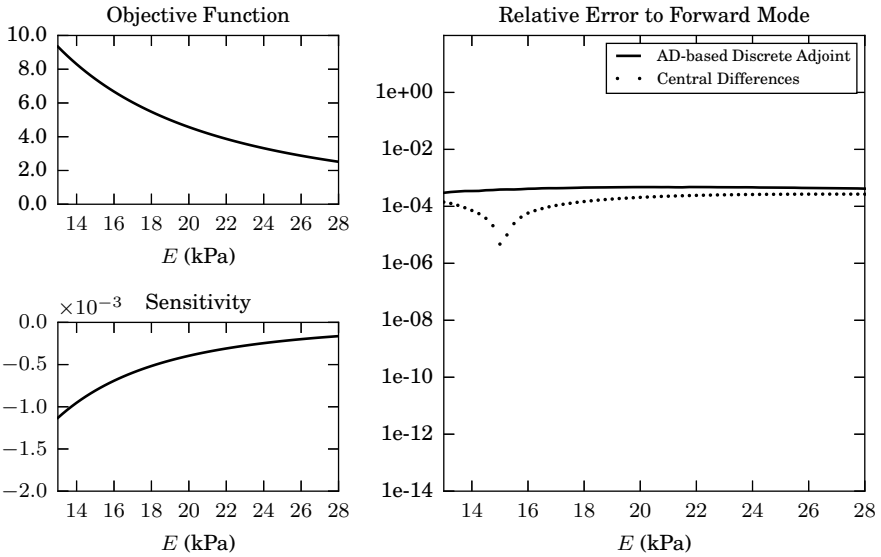

Figure 5: Objective function, sensitivity and relative error between AD-based Discrete Adjoint and Central Differences with respect to Forward Mode.

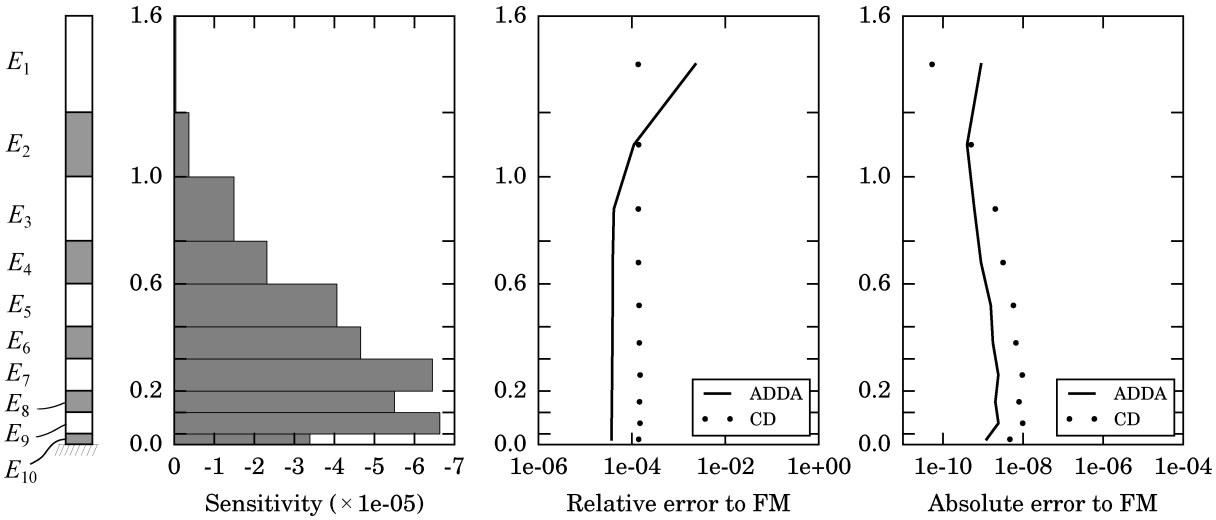

Figure 6: Far left: design variables. Left: Sensitivities for the design vector. Center: Relative error with the forward mode of AD. Right: Absolute error of the same magnitude.

4 CONCLUSIONS

This paper has described a new approach to compute derivatives in computational aeroelasticity. The method puts no restrictions to the governing equations on fluid and structure and it has been implemented for problems involving the (compressible) Navier-Stokes equations coupled with a geometrically-nonlinear structure (modelled using solid elements). A numerical example on a simple structure undergoing large deformations has shown the excellent performance of the approach.

5 REFERENCES

[1] Economon, T., Palacios, F., Copeland, S., et al. (2016). SU2: An open-source suite for multiphysics simulation and design. *AIAA Journal*, 54(3), 828–846. doi: 10.2514/1.J053813.

[2] Dou, S. (2015). *Gradient-based optimization in nonlinear structural dynamics*. Ph.D. thesis, Technical University of Denmark.

[3] Kenway, G., Kennedy, G., and Martins, J. (2014). Scalable parallel approach for high-fidelity steady-state aeroelastic analysis and adjoint derivative computations. *AIAA Journal*, 52(5), 935–951. doi:10.2514/1.J052255.

[4] Haghighat, S., Martins, J. R. R. A., and Liu, H. H. T. (2012). Aeroservoelastic design optimization of a flexible wing. *Journal of Aircraft*, 49(2), 432–443. doi:10.2514/1.C031344.

[5] Lund, E., Møller, H., and Jakobsen, L. (2003). Shape design optimization of stationary fluid-structure interaction problems with large displacements and turbulence. *Structural and Multidisciplinary Optimization*, 25(5-6), 383–392. doi:10.1007/s00158-003-0288-5.

[6] Barcelos, M. and Maute, K. (2008). Aeroelastic design optimization for laminar and turbulent flows. *Computer Methods in Applied Mechanics and Engineering*, 197(19-20), 1813–1832. doi:10.1016/j.cma.2007.03.009.

[7] Griewank, A. and Walther, A. (2008). *Evaluating Derivatives*. Society for Industrial and Applied Mathematics, second ed. doi:10.1137/1.9780898717761.

[8] Albring, T., Sagebaum, M., and Gauger, N. (2015). Development of a consistent discrete adjoint solver in an evolving aerodynamic design framework. In *16th AIAA/ISSMO Multidisciplinary Analysis and Optimization Conference*. Dallas, Texas, 22-26 June.

[9] Sanchez, R., Palacios, R., Economon, T., et al. (2016). Towards a Fluid-Structure Interaction solver for problems with large deformations within the open-source SU2 suite. In *57th AIAA/ASCE/AHS/ASC Structures, Structural Dynamics, and Materials Conference*. San Diego, California, 4-8 Jan.

[10] Farhat, C., Lesoinne, M., and Maman, N. (1995). Mixed explicit/implicit time integration of coupled aeroelastic problems: three-field formulation, geometric conservation and distributed solution. *International Journal for Numerical Methods in Fluids*, 21(10), 807–835.

[11] Maute, K., Nikbay, M., and Farhat, C. (2003). Sensitivity analysis and design optimization of three-dimensional non-linear aeroelastic systems by the adjoint method. *International Journal for Numerical Methods in Engineering*, 56(6), 911–933. doi:10.1002/nme.599.

[12] Arora, J. S. (2012). *Introduction to Optimum Design*. Boston Academic Press, 3rd ed.

[13] Hogan, R. (2014). Fast reverse-mode automatic differentiation using expression templates in C++. *ACM Transactions on Mathematical Software*, 40(4). doi:10.1145/2560359.

COPYRIGHT STATEMENT